

## Integrated Image Reconstruction and Gradient Nonlinearity Correction

Joshua D. Trzasko<sup>1</sup>, Shengzhen Tao<sup>1</sup>, Yunhong Shu<sup>1</sup>, Armando Manduca<sup>1</sup>, and Matt A. Bernstein<sup>1</sup>

<sup>1</sup>Mayo Clinic, Rochester, MN, United States

**Target Audience:** Image reconstruction scientists and physicists involved in quality control.

**Purpose:** Due to engineering limitations, the gradient fields used for spatial encoding in clinical magnetic resonance imaging (MRI) are never truly linear over the imaging field-of-view (FOV). As standard MRI signal models presume gradient linearity, reconstructed images exhibit geometric distortion unless gradient deviations are properly accounted for. Given *a priori* knowledge of the gradient field, geometric distortion due to gradient nonlinearity is typically corrected via image-domain interpolation [1,2]. Although this retrospective approach, commonly termed gradient distortion correction or “GradWarp”, is straightforward, it does not explicitly account for the effects of finite sampling, undersampling, or noise, and may consequently degrade spatial resolution. In this work, we propose a correction strategy that accounts for gradient nonlinearity during – rather than after – k-space to image reconstruction. Although prospective correction has been considered in situations when gradients are intentionally distorted for encoding purposes (e.g., PATLOC [3]), this approach has not been considered for the more common scenario where ideally linear gradients are not performing as desired. As will be shown, prospective compensation lessens the tradeoff between geometric accuracy and spatial resolution.

**Methods:** In the presence of gradient nonlinearity, the measured MRI signal can be modeled as  $\mathbf{g}[\mathbf{k}] = \int_{\Omega} \mathbf{f}(\vec{x}) e^{j\vec{\omega}[\mathbf{k}] \cdot \vec{\Delta}(\vec{x})} d\vec{x} + \mathbf{n}[\mathbf{k}]$  (Eq. 1), where  $\mathbf{f}$  is the (continuous) target signal,  $\vec{x}$  denotes (true) spatial position,  $\vec{\omega}$  is the sample frequency,  $\vec{\Delta}$  is the (assumed *a priori* known) spatial distortion function due to gradient nonlinearity, and  $\mathbf{n}$  is complex Gaussian noise. As only a finite number of samples is collected, the target signal,  $\mathbf{f}$ , is approximated via finite series representation,  $\mathbf{f}(\vec{x}) \approx \sum_{i \in \Theta} \mathbf{u}[i] \mathbf{b}(\vec{x} - \vec{r}[i])$ , where  $\mathbf{u}$  are display coefficients,  $\mathbf{b}$  is the voxel model, and  $\vec{r}$  is voxel position.

Presuming a Dirac delta voxel model, (Eq. 1) resorts to  $\mathbf{g}[\mathbf{k}] \approx \sum_{i \in \Theta} \mathbf{u}[i] e^{j\vec{\omega}[\mathbf{k}] \cdot \vec{\Delta}(\vec{r}[i])} + \mathbf{n}[\mathbf{k}] = \mathbf{A}\mathbf{u}[\mathbf{k}] + \mathbf{n}[\mathbf{k}]$  (Eq. 2). The forward operator,  $\mathbf{A}$ , can be efficiently implemented for Cartesian and non-Cartesian sampling using type-1 and type-3 non-uniform fast Fourier transforms (NUFFT) [4], respectively, and readily embedded into any reconstruction method based on solving an optimization problem of the following abstract form:  $\{\hat{\mathbf{u}}\} = \arg \min \{\lambda \mathbf{P}(\mathbf{u}) + \|\mathbf{A}\mathbf{u} - \mathbf{g}\|_F^2\}$  (Eq. 3), where  $\mathbf{P}(\cdot)$  is a penalty functional. To demonstrate the proposed strategy, the American College of Radiology (ACR) quality assurance (QA) phantom was scanned at 3.0 T (GE v16, T<sub>1</sub>-weighted RF spin echo, FOV=25cm, Nx=Ny=256, 11 5 mm slices, TR/TE = 500/20ms, FA=90°, ZOOM gradients, 8-channel array). Raw complex MRI data was then retrospectively 2x undersampled (randomly) along the phase-encoded direction. CLEAR [5] (iter=50, blocksize=8,  $\lambda=1e5$ ) was adopted as the reconstruction platform, such that  $\mathbf{P}$  in Eq. 3 was defined as a locally low-rank (LLR) penalty functional.  $\mathbf{A}$  was implemented using a type-1 NUFFT with 1.25x oversampling and a width  $J=5$  Kaiser-Bessel kernel. Image reconstruction was performed assuming no spatial distortion (i.e.,  $\vec{\Delta}(\vec{x}) = \vec{x}$ ) and with a distortion map generated using vendor-provided gradient (i.e.,  $\vec{\Delta}(\vec{x}) \neq \vec{x}$ ). As a baseline for comparison, geometric distortion in the former reconstruction was also retrospectively corrected via image-domain interpolation (cubic spline).

**Results:** Fig. 1 shows reconstruction results for two slices of the ACR phantom dedicated for assessing geometric accuracy and spatial resolution. The results assert that retrospective (“CLEAR+GradWarp”) and prospective (“Proposed”) correction both effectively combat geometric image distortion evident in the uncorrected image (“CLEAR”), but retrospective correction also degrades spatial resolution during this correction while the proposed strategy does not. This difference is particularly evident when comparing the 1.0/1.1 mm resolution inserts of different results.

**Discussion:** Gradient nonlinearity correction is routinely performed in clinical MRI, and any improvements to this process may offer widespread benefit. The ability of prospective correction to preserve spatial resolution may be particularly beneficial for longitudinal MRI studies [6] looking for subtle image changes, and in the design of novel scanner architectures based on fast but sensitive gradients systems [7]. That the proposed approach readily integrates into existing MRI reconstruction strategies should also facilitate its adoption; however, additional effort is needed to further reduce the computational cost of the added NUFFT operations.

**Conclusion:** Prospectively accounting for distortion due to gradient nonlinearity during – rather than after – k-space to image reconstruction lessens the tradeoff between geometric accuracy and spatial resolution inherent to retrospective correction strategies.

**References:** [1] Glover et al., US Patent 4591789, 1986; [2] Janke et al., MRM 52:115-22, 2004; [3] Knoll et al., MRM 70: 40-52, 2013; [4] Greengard and Lee, SIAM Rev 46:443-54, 2004; [5] Trzasko and Manduca, ISMRM 2012, 517; [6] Jack et al., JMRI 27:685-91, 2008; [7] Mathieu et al., ISMRM 2013, 2708.

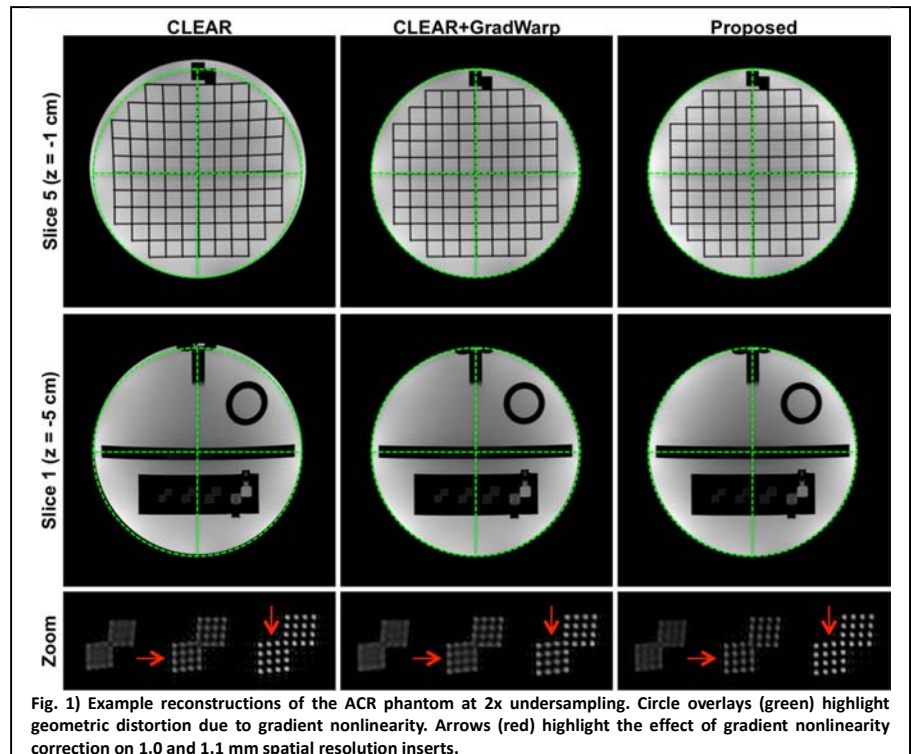


Fig. 1) Example reconstructions of the ACR phantom at 2x undersampling. Circle overlays (green) highlight geometric distortion due to gradient nonlinearity. Arrows (red) highlight the effect of gradient nonlinearity correction on 1.0 and 1.1 mm spatial resolution inserts.